Piezoactuator Design Considering the Optimum Placement of FGM Piezoelectric Material

Ronny C. Carbonari[a], Shinji Nishiwaki[b], Glaucio H. Paulino[c], and Emílio C. Nelli Silva[a]

[a]Department of Mechatronics ad Mechanical Systems Engineering
Escola Politécnica da Universidade de São Paulo
Av. Prof. Mello Moraes, 2231, São Paulo - SP - 05508-900, Brazil
[b]Department of Aeronautics and Astronautics
Kyoto University
Sakyo-Ku, Kyoto, 606-8501, Japan
[c] Newmark Laboratory, Department of Civil and Environmental Engineering, University of Illinois at Urbana-Champaign,
Newmark Laboratory, 205 North Mathews Avenue, Urbana, IL 61801, U.S.A.

ABSTRACT

Functionally Graded Materials (FGMs) possess continuous variation of material properties and are characterized by spatially varying microstructures. Recently, the FGM concept has been explored in piezoelectric materials to improve properties and to increase the lifetime of piezoelectric actuators. Elastic, piezoelectric, and dielectric properties are graded along the thickness of a piezoceramic FGM. Thus, the gradation of piezoceramic properties can influence the performance of piezoactuators, and an optimum gradation can be sought through optimization techniques. However, the design of these FGM piezoceramics are usually limited to simple shapes. An interesting approach to be investigated is the design of FGM piezoelectric mechanisms which essentially can be defined as a FGM structure with complex topology made of piezoelectric and non-piezoelectric material that must generate output displacement and force at a certain specified point of the domain and direction. This can be achieved by using topology optimization method. Thus, in this work, a topology optimization formulation that allows the simultaneous distribution of void and FGM piezoelectric material (made of piezoelectric and non-piezoelectric material) in the design domain, to achieve certain specified actuation movements, will be presented. The method is implemented based on the SIMP material model where fictitious densities are interpolated in each finite element, providing a continuum material distribution in the domain. The optimization algorithm employed is based on sequential linear programming (SLP) and the finite element method is based on the graded finite element concept where the properties change smoothly inside the element. This approach provides a continuum approximation of material distribution, which is appropriate to model FGMs. Some FGM piezoelectric mechanisms were designed to demonstrate the usefulness of the proposed method. Examples are limited to two-dimensional models, due to FGM manufacturing constraints and the fact that most of the applications for such FGM piezoelectric mechanisms are planar devices. An one-dimensional constraint of the material gradation is imposed to provide more realistic designs.

Keywords: nanopositioners, MEMS, FGM, piezoelectric actuators, topology optimization, finite element analysis

Further author information: Emílio C. N. Silva
Ronny C. Carbonari: E-mail: ronny@usp.br, Telephone: +55 (11) 3091 9851
Emílio C. N. Silva: E-mail: ecnsilva@usp.br, Telephone: +55 (11) 3091 9754
Shinji Nishiwaki: E-mail: shinji@prec.kyoto-u.ac.jp, Telephone: +81 (75) 753 9186
Glaucio H. Paulino: E-mail: paulino@uiuc.edu, Telephone: +1 (217) 333-3817

Modeling, Signal Processing, and Control for Smart Structures 2007, edited by Douglas K. Lindner
Proc. of SPIE Vol. 6523, 65230C, (2007) · 0277-786X/07/$18 · doi: 10.1117/12.715411

1. INTRODUCTION

Piezoelectric micro-tools offer significant promise in a wide range of applications involving nanopositioning and micromanipulation.[1] For instance, piezoelectric positioners are applied to atomic force microscopes (AFM) and scanning tunneling microscopes (STM) for positioning the sample or the probe, respectively[2,3]; piezoelectric microgrippers are applied to micromanipulation,[4] cell manipulation and microsurgery.[5] The micro-tools usually consist of multi-flexible structures actuated by two or more functionally graded piezoceramic devices that must generate different output displacements and forces at different specified points of the domain and on different directions. Thus, the development of these piezoelectric micro-tools require the design of actuated compliant mechanisms[6] that can perform detailed specific movements. Although the design of such micro-tools is complicated due to the coupling between movements generated by various piezoceramics, it can be realized by means of topology optimization[7,8] which even allows the simultaneous search for an optimal topology of a flexible structure as well as the optimal positions of the piezoceramics in the design domain, to achieve certain specified actuation movements.[9]

Functionally Graded Materials (FGMs) are special materials that possess continuously graded properties and are characterized by spatially varying microstructures created by nonuniform distributions of the reinforcement phase as well as by interchanging the role of reinforcement and matrix (base) materials in a continuous manner.[10] The smooth variation of properties may offer advantages such as local reduction of stress concentration and increased bonding strength.

Topology optimization is a powerful structural optimization method that seeks an optimal structural topology design by determining which points of space should be solid and which points should be void (i.e. no material) inside a given domain.[11] However, the binary (0–1) design is an ill-posed problem and a typical way to seek a solution for topology optimization problems is to relax the problem by defining a material model that allows for intermediate (composites) property values. In this sense, the relaxation yields a continuous material design problem that no longer involves a discernible connectivity. Typically, it is an improperly formulated (ill-posed) topology optimization problem for which no optimum solution exists (0-1 design). A topology solution can be obtained by applying penalization coefficients to the material model to recover the 0-1 design (and thus, a discernible connectivity), and some gradient control of material distribution, such as a filter for example.[11]

The relaxed problem is strongly related to the functionally graded material (FGM) design problem, which essentially seeks a continuous transition of material properties.[10] In contrast, while the 0–1 design problem does not admit intermediate values of design variables, the FGM design problem does admit solutions with intermediate values of the material field.

Due to the attractive possibilities of tailoring the material properties, some researchers have applied optimization methods to design FGMs.[12] The application of a generic optimization method to tailor material property gradation has been proposed by Paulino and Silva[13] who applied topology optimization to solve the problem of maximum stiffness design.

Recently, the concept of functionally graded materials (FGMs) has been explored in piezoelectric materials to improve their properties and increase the lifetime of piezoelectric actuators.[14] Usually, elastic, piezoelectric, and dielectric properties are graded along the thickness of an FGM piezoceramic. Previous studies[14,15] have shown that the gradation of piezoceramic properties can influence the performance of piezoactuators, such as generated output displacements. This suggests that optimization techniques can be applied to take advantage of the property gradation variation to improve the FGM piezoactuator performance.

However, the design of these FGM piezoactuators are usually limited to simple shapes. An interesting approach to be investigated is to mix the concept of FGM with micro-tools, that is, to design FGM piezoelectric mechanisms which essentially can be defined as a FGM structure with complex topology made of piezoelectric and non-piezoelectric material that must generate output displacement and force at a certain specified point of the domain and direction. This can be achieved by using topology optimization method.

Thus, the objective of this work is to develop a topology optimization formulation that allows the simultaneous distribution of void and FGM piezoelectric material (made of piezoelectric and non-piezoelectric material) in the design domain, to achieve certain specified actuation movements. Two design problems are considered simultaneously: the optimum design of the piezoceramic property gradation in the FGM piezoceramic domain,

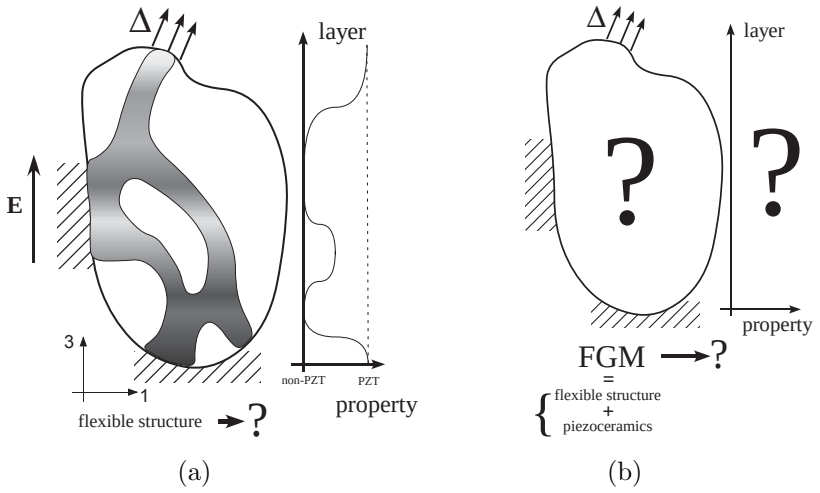

Figure 1. (a) FGM piezoelectric mechanism concept; (b) FGM piezoelectric device design problem considering the simultaneous distribution of FGM piezoceramic and void in the design domain.

and the design of the FGM structural topology. Figure 1 illustrates the concept of FGM piezoelectric devices proposed in this work.

The optimization problem is posed as the design of a FGM structure, as well as its property gradation that maximizes output displacement or output force in a specified direction and point of the domain, while minimizing the effects of movement coupling.[8] The method is implemented based on the solid isotropic material with penalization (SIMP) model where fictitious densities are interpolated at each finite element, providing a continuous material distribution in the domain. The optimization algorithm employed is based on sequential linear programming (SLP).[16, 17] Since the position of piezoceramic are not known "a priori" an independent electrical excitation is considered for each finite element which is equivalent to a constant applied electric field.[9] This decouples the electrical and mechanical problem, however, the dielectric properties are not taken into account in the design problem.

Thus, this formulation contributes to increase the design flexibility of these devices allowing the design of novel types of FGM piezoactuators for different applications. Some FGM piezoelectric mechanisms were designed to demonstrate the usefulness of the proposed method. Although the presented examples are limited to two-dimensional models (2D plane stress), this is appropriate since most of the applications for such FGM piezoactuators are planar devices. An one-dimensional constraint of the FGM gradation is imposed to provide more realistic designs. The use of topology optimization for the design of FGM piezoactuators is a novel approach that has the potential to dramatically broaden the applied range of such devices, especially in the field of smart structures.

2. FINITE ELEMENT FGM PIEZOELECTRIC MODELING

The micro-tools considered here operate in quasi-static or low-frequency modes (inertia effects are neglected). When a non-piezoelectric conductor material and a piezoceramic material are distributed in the piezoceramic domain, the electrode positions are not known "a priori", as discussed ahead. Thus, the electrical excitation is given by an applied electric field[9] ($\nabla\phi$=constant). In this case, all electrical degrees of freedom are specified in the FE problem, and thus the linear finite element (FE) matrix formulation of the equilibrium equations for the piezoelectric medium is given by[18]:

$$\begin{bmatrix} \mathbf{K_{uu}} & \mathbf{K_{u\phi}} \\ \mathbf{K}^t_{\mathbf{u}\phi} & -\mathbf{K}_{\phi\phi} \end{bmatrix} \begin{Bmatrix} \mathbf{U} \\ \mathbf{\Phi} \end{Bmatrix} = \begin{Bmatrix} \mathbf{F} \\ \mathbf{Q} \end{Bmatrix} \Longrightarrow [\mathcal{K}]\{\mathcal{U}\} = \{\mathcal{Q}\} \Longrightarrow \begin{matrix} [\mathbf{K_{uu}}]\{\mathbf{U}\} = \{\mathbf{F}\} - [\mathbf{K_{u\phi}}]\{\mathbf{\Phi}\} \\ \left[\mathbf{K}^t_{\mathbf{u}\phi}\right]\{\mathbf{U}\} = \{\mathbf{Q}\} + [\mathbf{K}_{\phi\phi}]\{\mathbf{\Phi}\} \end{matrix} \tag{1}$$

since $\{\mathbf{\Phi}\}$ is specified. $\mathbf{K_{uu}}$, $\mathbf{K_{u\phi}}$, and $\mathbf{K}_{\phi\phi}$ denote the stiffness, piezoelectric, and dielectric matrices, respectively, and $\mathbf{F}$, $\mathbf{Q}$, $\mathbf{U}$, and $\mathbf{\Phi}$ are the nodal mechanical force, nodal electrical charge, nodal displacements, and nodal electric potential vectors, respectively.[18]

In the case of FGM piezoceramics, the properties change continuously inside the piezoceramic domain, which means that they can be described by some continuous function of position $\mathbf{x}$ in the piezoceramic domain, that is:

$$\mathbf{C} = \mathbf{C}(\mathbf{x});\ \mathbf{e} = \mathbf{e}(\mathbf{x});\ \boldsymbol{\epsilon}^S = \boldsymbol{\epsilon}^S(\mathbf{x}) \tag{2}$$

From the mathematical definitions of $\mathbf{K_{uu}}$, $\mathbf{K_{u\phi}}$, and $\mathbf{K}_{\phi\phi}$, these material properties must remain inside the matrices integrals and be integrated together by using the graded finite element concept[19] where properties are continuously interpolated inside each finite element based on property values at each finite element node. An attempt to approximate the continuous change of material properties by a stepwise function where a property value is assigned for each finite element may result in less accurate results with undesirable discontinuities of the stress and strain fields.

Therefore, the mechanical and electrical problems are decoupled, and only the upper problem of Equation (1) needs to be directly solved. Essentially, the optimization problem is based on the mechanical problem. As a consequence, the dielectric properties do not influence the design.

3. DESIGN PROBLEM FORMULATION

For topology optimization[11] numerical implementation, we are considering the continuous distribution of the design variable inside the finite element by interpolating it using the FE shape functions.[20] In this case, the design variables are defined for each element node. This formulation, known as CAMD ("Continuous Approximation of Material Distribution") seems to reduce instabilities, such as checkerboard of the material layout designs.[20]

We are interested in a simultaneous distribution of void, and FGM piezoelectric material in the design domain, and thus, the following material model is proposed based on an simple extension of the SIMP ("Solid Isotropic Material with Penalization") model[11] considering CAMD concept:

$$\mathbf{C} = \rho_1^{p_{c1}}\left[\rho_2\mathbf{C}_1 + (1-\rho_2)\,\mathbf{C}_2\right] + (1-\rho_1^{p_{c1}})\,\mathbf{C}_{\text{void}} \tag{3}$$

$$\mathbf{e} = \rho_1^{p_{c1}}\left[\rho_2\mathbf{e}_1 + (1-\rho_2)\,\mathbf{e}_2\right], \tag{4}$$

where ρ_1 and ρ_2 are pseudo-density function representing the amount of material at each point of the domain. These design variables can assume different values at each finite element node. Thus, $\rho_1 = 1.0$ denotes FGM material and $\rho_1 = 0.0$ denotes void, and $\rho_2 = 1.0$ denotes piezoelectric material **type 1** or $\rho_2 = 0.0$ denotes piezoelectric material **type 2**. $\mathbf{C}$ and $\mathbf{e}$ are stiffness and piezoelectric tensor properties, respectively, of the material. The tensors $\mathbf{C}_j$ and $\mathbf{e}_j$ are related to the stiffness and piezoelectric properties for piezoelectric material type j ($j = 1, 2$), respectively. $\mathbf{C}_{\text{void}}$ is the tensor related to void stiffness property. Eventually, the piezoelectric material type 2 can be substituted by the flexible structure material (non-piezoelectric material, such as Aluminum, for example), and in this case $\mathbf{e}_2 = \mathbf{0}$. These are the properties of basic materials that are distributed in the piezoceramic domain. The dielectric properties are not considered because a constant electric field is applied to the design domain as electrical excitation, and as explained in Section 4, this approach decouples the electrical and mechanical problems eliminating the influence of dielectric properties in the optimization problem. p_{c1} is a penalization factor to recover the discrete design, and its value varies from 0 to 3. For a discretized domain into finite elements, Equations (3) and (4) are considered for each element node, and the material properties inside each finite element are given by functions of $\mathbf{x}$ ($\rho_1(\mathbf{x})$ and $\rho_2(\mathbf{x})$) according to the CAMD concept. This formulation leads to a continuous distribution of material along the design domain. Thus, by finding the nodal values of the unknown ρ_1 and ρ_2 function, we are indirectly finding the optimum material distribution functions, which are described by Equation (2).

In this work, the piezoceramic electrodes are not known "a priori", and, thus, an electric field is applied as electrical excitation. Essentially, the objective function is defined in terms of generated output displacements for a certain applied electric field to the design domain. The mean transduction ($L_2(\mathbf{u}_1, \phi_1)$) concept is related

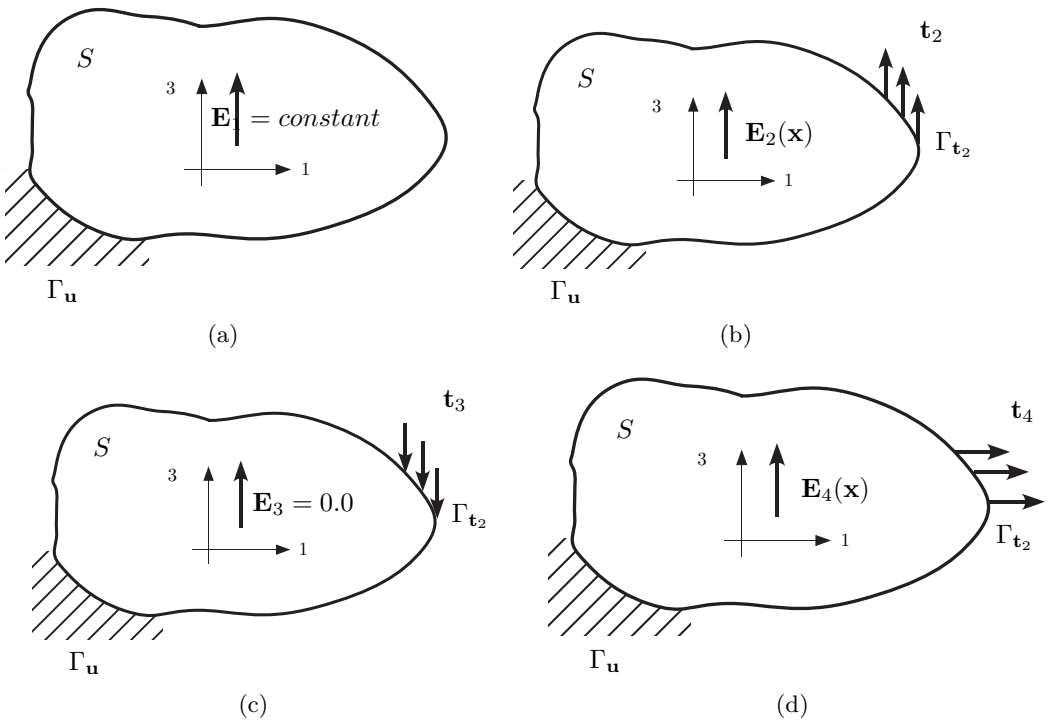

Figure 2. Load cases for calculation of: mean transduction (Figures 2(a) and 2(b)), mean compliance (2(c)), and displacement coupling constraint function (Figures 2(a) and 2(d)). Here, $\mathbf{E}_i = -\nabla\phi_i$ denotes the electrical field associated with load case i.

to the electromechanical conversion represented by the displacement generated in region $\Gamma_{\mathbf{t}_2}$ along a specified direction due to an input electrical excitation in the medium (in this work, $\mathbf{E}_1$ is prescribed). Thus, the larger $L_2(\mathbf{u}_1, \phi_1)$, the larger the displacement generated in this region along the $\mathbf{t}_2$ direction due to an applied electric field to the medium. Considering d_i and ϕ_i the electrical displacement and electrical potential related to load case i, respectively, the mean transduction is defined by[21]:

$$L_2(\mathbf{u}_1, \phi_1) = \int_{\Gamma_{t_2}} \mathbf{t}_2\mathbf{u}_1\, d\Gamma + \int_{\Gamma_{d_2}} d_2\phi_1\, d\Gamma = \int_{\Gamma_{t_2}} \mathbf{t}_2\mathbf{u}_1\, d\Gamma, \tag{5}$$

as $d_2 = 0$ in this problem. Therefore, the maximization of output displacement generated in a region $\Gamma_{\mathbf{t}_2}$ is obtained by maximizing the mean transduction quantity ($L_2(\mathbf{u}_1, \phi_1)$). The load cases considered for calculation of mean transduction are shown in instances 2(a) and 2(b) of Figure 2 .

However, the optimum solution obtained considering only the maximization of mean transduction may be a structure with very low stiffness. The piezoactuator must resist to reaction forces (in region $\Gamma_{\mathbf{t}_2}$) generated by a body that the piezoactuator is trying to move or grab. Therefore, the mean compliance must be minimized to provide enough stiffness (see Figure 2(c)). The mean compliance is calculated by considering the load case described in case 2(c) of Figure 2 where a traction $\mathbf{t}_3 = -\mathbf{t}_2$ is applied to region $\Gamma_{\mathbf{t}_2}$ and the electric field is kept null inside the medium ($\mathbf{E}_3 = 0$). The displacement coupling constraint is obtained by minimizing the absolute value of the corresponding mean transduction related to undesired generated displacement. This will minimize an undesired displacement generated when an electric field is applied. Therefore, the mean transduction $L_4(\mathbf{u}_1, \phi_1)$ related to the displacement normal to the desired displacement at $\Gamma_{\mathbf{t}_2}$ must be minimized (see Figure 2(d)), and it is calculated by using Equation 2, however, considering a load case described in case 2(d) of Figure 2 instead, where a traction $\mathbf{t}_4$, normal to $\mathbf{t}_2$, is applied to region $\Gamma_{\mathbf{t}_2}$.[8]

To properly combine the mean transduction, mean compliance maximization, and coupling constraint minimization, a multi-objective function is constructed to find an appropriate optimal solution that can incorporate

all design requirements. The following multi-objective function is proposed to combine all these optimization aspects[9]:

$$\begin{aligned}\mathcal{F}(\rho_1,\rho_2) &= w * \ln\left[L_2(\mathbf{u}_1,\phi_1)\right] - \\ &- \frac{1}{2}(1-w)\ln\left[L_3(\mathbf{u}_3,\phi_3)^2 + \beta L_4(\mathbf{u}_1,\phi_1)^2\right],\end{aligned} \tag{6}$$

where w is a weight coefficient ($0 \leq w \leq 1$). The coefficient w allows control of the contributions of mean transduction (Equation 2), mean compliance, and displacement coupling in the design. Accordingly, the final optimization problem is defined as:

$$\begin{array}{ll} \underset{\rho_1(\mathbf{x}),\rho_2(\mathbf{x})}{Maximize}: & \mathcal{F}(\rho_1,\rho_2) \\ subject\ to: & \text{Equilibrium equations for different load cases} \\ & 0 \leq \rho_1 \leq 1;\ 0 \leq \rho_2 \leq 1; \\ & \Theta_1(\rho) = \int_S \rho_1 dS - \Theta_{1S} \leq 0;\ \Theta_2(\rho) = \int_S \rho_2 dS - \Theta_{2S} \leq 0 \end{array} \tag{7}$$

Here S denotes the design domain, Θ_1 is the volume of this design domain, and Θ_{1S} is an upper-bound volume constraint defined to limit the maximum amount of material used to build the FGM coupling structure. Moreover, Θ_2 is the volume related to ρ_2 design variable, and Θ_{2S} is an upper-bound volume constraint defined to limit ρ_2 values when optimizing the FGM gradation function. The other constraints are equilibrium equations for the piezoelectric medium considering different load cases. The equilibrium equations are solved separately from the optimization problem. They are stated in the problem to indicate that, whatever topology is obtained, it must satisfy the equilibrium equations.

4. NUMERICAL IMPLEMENTATION

The continuum distribution of design variables $\rho_1(\mathbf{x})$ and $\rho_2(\mathbf{x})$ are given by the functions[20]

$$\rho_1(\mathbf{x}) = \sum_{I=1}^{n_d} \rho_{1I} N_I(\mathbf{x});\ \rho_2(\mathbf{x}) = \sum_{I=1}^{n_d} \rho_{2I} N_I(\mathbf{x}) \tag{8}$$

where ρ_{1I} and ρ_{2I} are nodal design variables, N_I is the finite element shape function that must be selected to provide non-negative values of the design variables, and n_d is the number of nodes at each finite element. The design variables ρ_{1I} and ρ_{2I} can assume different values at each node of the finite element.

Due to the definition of Equation (8), the material property functions (Equations (3) and (4)) also have a continuum distribution inside the design domain. Thus, considering the mathematical definitions of the stiffness and piezoelectric matrices of Equation (1), the material properties must remain inside the integrals and be integrated together by means of the graded finite element concept.[19] The finite element equilibrium Equation (1) is solved considering 4-node isoparametric finite elements under either plane stress or plane strain assumptions.

When a non-piezoelectric conductor material (usually a metal, such as Aluminum) is considered in Equations (3) and (4), a relevant problem to be solved is how to define the piezoceramic electrodes. If only different types of piezoelectric materials are considered, the position of electrodes surface is known and is defined by the piezoceramic domain geometry. However, if a non-piezoelectric conductor material (for example, Aluminum) is also distributed in the piezoceramic design domain, we cannot define "a priori" the position of the piezoceramic electrodes because we do not know where the piezoceramic is located in the design domain. To circumvent this problem, we consider the electrical problem independently for each finite element of the piezoceramic domain by defining a pair of electrodes at each finite element, that is, each finite element has its own electrical degrees of freedom as illustrated by Figure 3.

Thus, each finite element has 4 electrical degrees of freedom given by $[\phi_a, \phi_b, \phi_c, \phi_d]$ (nodes are ordered counterclockwise starting from the upper right corner of each finite element) considering that one of the electrodes

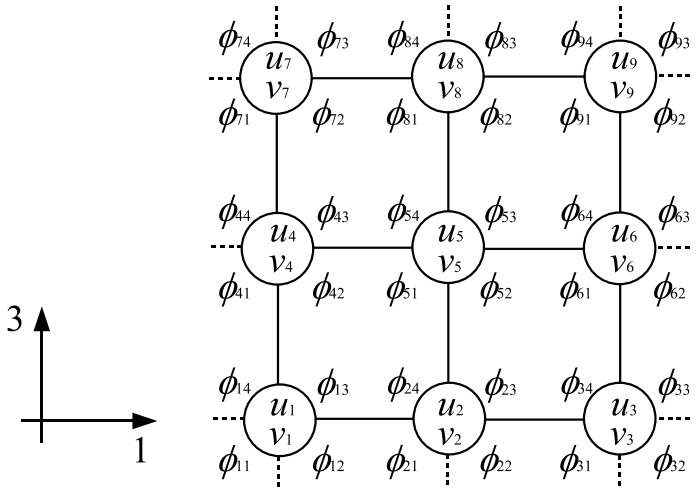

Figure 3. Finite elements with their corresponding electrical degrees of freedom. Here, u_i and v_i denote the node i horizontal and vertical displacement, respectively; and ϕ_{ij} denotes the j-th potential at the i-th node.

is grounded. Electrical voltage ϕ_0 is applied to the two upper nodes, and thus, the four electrical degrees of freedom are prescribed at each finite element, as follows ($[\phi_0, \phi_0, 0, 0]$).[9] This is equivalent to applying a constant electrical field along the 3-direction in the design domain (see Figure 3). In this case, all electrical degrees of freedom are prescribed in the FE problem.

By means of the FE matrix formulation of equilibrium, Equation (1), the discrete forms of mean transduction, Equation (5), and mean compliance for actuation movement i can be calculated numerically.

The discretized form of the optimization problem given by Equation (7) is restated as:

$$
\begin{array}{lll}
\underset{\rho_{1I},\rho_{2I}}{Maximize}: & \mathcal{F}\left(\rho_{1I},\rho_{2I}\right) & \\
subject\ to: & \{\mathbf{F}_3\} = -\{\mathbf{F}_2\} \qquad (\Gamma_{\mathbf{t}_3} = \Gamma_{\mathbf{t}_2}) & \\
 & \{\mathbf{F}_4\}^t \{\mathbf{F}_2\} = 0 \qquad (\Gamma_{\mathbf{t}_4} = \Gamma_{\mathbf{t}_2}) & \\
 & [\mathcal{K}_1]\{\mathcal{U}_1\} = \{\mathcal{Q}_1\} & [\mathcal{K}_2]\{\mathcal{U}_2\} = \{\mathcal{Q}_2\} \\
 & [\mathcal{K}_3]\{\mathcal{U}_3\} = \{\mathcal{Q}_3\} & [\mathcal{K}_2]\{\mathcal{U}_4\} = \{\mathcal{Q}_4\} \\
 & 0 \le \rho_{1I} \le 1;\ 0 \le \rho_{2I} \le 1 & I = 1..N_e \\
 & \sum_{I=1}^{NE} \int_{S_I} \rho_1 dS_I - \Theta_{1S} \le 0 & \\
 & \sum_{J=1}^{NE} \int_{S_J} \rho_2 dS_J - \Theta_{2S} \le 0 &
\end{array}
\tag{9}
$$

where the integrals in the volume constraint expressions are evaluated by using Gauss quadrature (4 points) and considering Equation (8). The parameter N_e is the number of nodes in the design design domain. Moreover, NE denotes the number of elements in the design domain. The matrices $[\mathcal{K}_1]$ and $[\mathcal{K}_3]$ are reduced forms of the matrix $[\mathcal{K}_2]$ considering non-zero and zero specified voltage degrees of freedom (applied electric field) at the piezoceramic domain, respectively. The initial domain is discretized by finite elements and the design variables ($\rho_1$and ρ_2) are the values of ρ_{1I} and ρ_{2J} are defined at each finite element node in the design domain.

A flow chart of the optimization algorithm describing the steps involved is shown in Figure 4. The software was implemented using the C language.

The mathematical programming method called Sequential Linear Programming (SLP) is applied to solve the optimization problem since there are a large number of design variables, and different objective functions and constraints.[16,17] The linearization of the problem at each iteration requires the sensitivities (gradients) of the

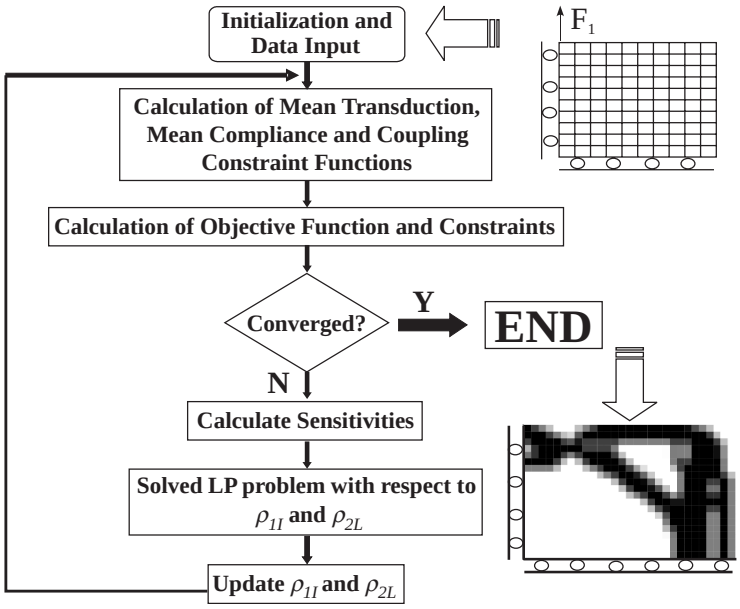

Figure 4. Flow chart of optimization procedure (LP means linear programming).

Table 1. Material Properties of PZT5A.

c_{11}^E (10^{10} N/m^2)	12.1	e_{13} (C/m^2)	-5.4
c_{12}^E (10^{10} N/m^2)	7.54	e_{33} (C/m^2)	15.8
c_{13}^E (10^{10} N/m^2)	7.52	e_{15} (C/m^2)	12.3
c_{33}^E (10^{10} N/m^2)	11.1		
c_{44}^E (10^{10} N/m^2)	2.30		
c_{66}^E (10^{10} N/m^2)	2.10		

multi-objective function and constraints. These sensitivities depend on gradients of mean transduction and mean compliance functions in relation to ρ_{1I} and ρ_{2J}.

Suitable moving limits are introduced to assure that the design variables do not change by more than 5–15% between consecutive iterations. A new set of design variables ρ_{1I} and ρ_{2J} are obtained after each iteration, and the optimization continues until convergence is achieved for the objective function. The results are obtained using the continuation method where the penalization coefficient p_{c1} varies from 1 to 3 along the iterations. The continuation method alleviates the problem of multiple local minimum (or maximum).[11]

5. NUMERICAL RESULTS

Examples are presented to illustrate the design piezoelectric actuators using the proposed method. Once the idea is to simultaneously distribute void, and FGM piezoelectric no regions with predefined materials are specified in the design domain S. For all examples, the FGM piezoelectric is composed of piezoelectric material and Aluminum, and the material gradation is constrained to the 3 direction. Table (1) presents the piezoelectric material properties used in the simulations for all examples. $\mathbf{C}$ and $\mathbf{e}$ are the elastic and piezoelectric properties, respectively, of the medium. The Young's modulus and Poisson's ratio of Aluminum are equal to 70 GPa and 0.33, respectively. Two-dimensional isoparametric finite elements under plane-stress assumption are used in the finite element analysis.

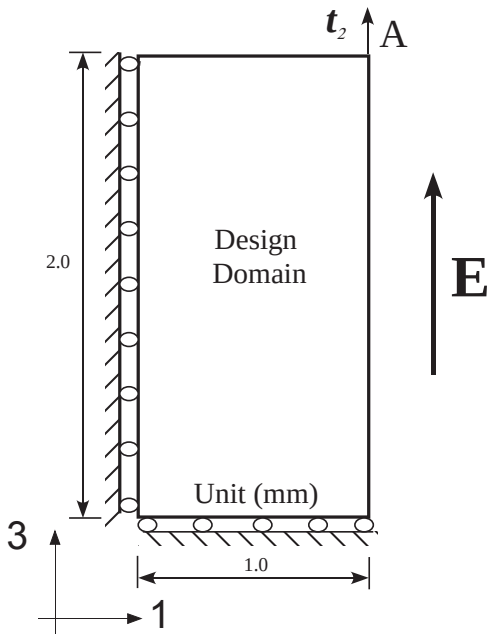

Figure 5. Design domain and load conditions.

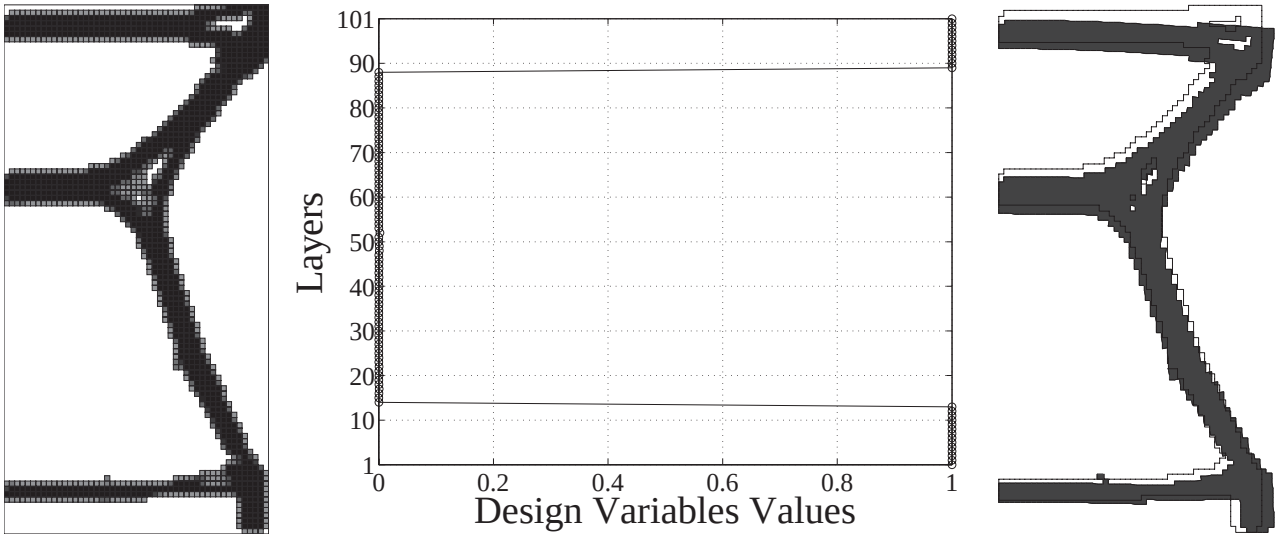

(a) (b) (c)

Figure 6. Result for $w = 0.7$ and $\beta = 0.0$; a) Optimal topology; b) Material gradation along 3 direction; c) Deformed configuration of interpreted topology.

The amount of electric field applied to the design domain is 500 V/mm (see Figure 5). The design domain for all examples is shown in Figure 5 which was discretized into 5000 finite elements. The mechanical and electrical boundary conditions are shown in the same figure. The FGM volume constraint and piezoelectric material volume constraint in the FGM are both equal to 25%. The initial values of design variables ρ_{1I} and ρ_{2I} are equal to 0.15, and the optimization problem starts in the feasible domain (all constraints satisfied). The results are shown by plotting the average density value. The final actuator configuration for all results is obtained by interpreting FGM topology by doing a simple threshold of pseudo-density value ρ_{1I}.

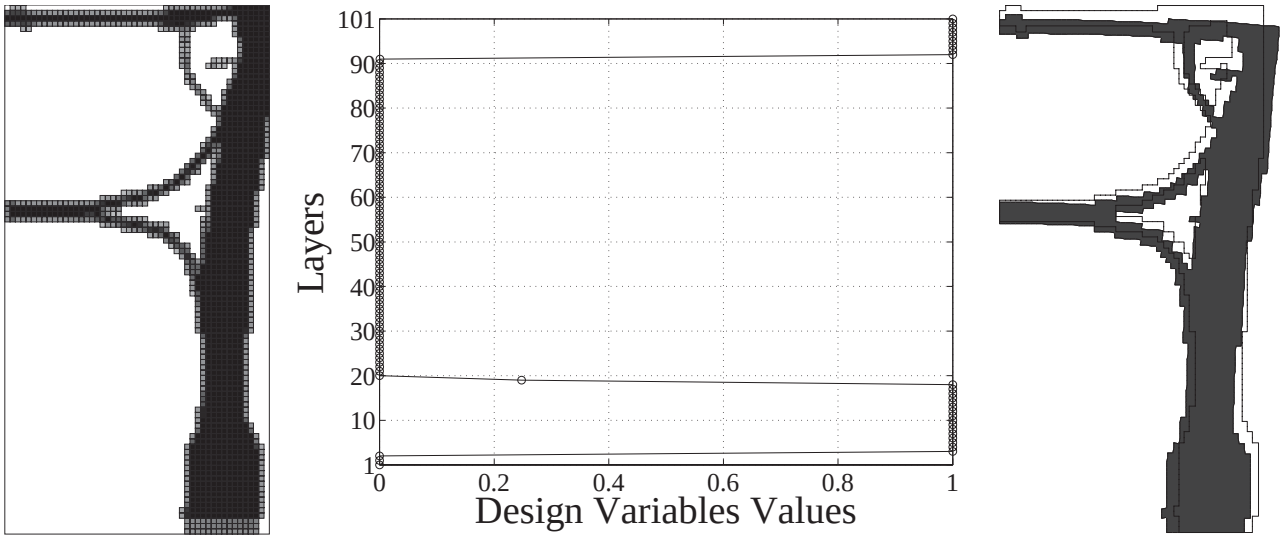

(a) (b) (c)

Figure 7. Result for $w = 0.5$ and $\beta = 0.0$; a) Optimal topology; b) Material gradation along 3 direction; c) Deformed configuration of interpreted topology.

In the first example, the topology optimization problem was solved considering $w = 0.7$. The β coefficient (see Equation 6) was set equal to 0.0 which means that the coupling constraint is not considered. The obtained piezoelectric FGM topology is shown in Figure 6(a). The graphic shown in Figure 6(b) describes the material gradation in the FGM domain along the 3 direction. A clear contrast among piezoelectric FGM topology and void could be obtained. However, the optimization tends to give results with a steep material gradation in the FGM domain. The piezoceramic is distributed in the upper and lower parts of the design domain. The corresponding deformed configuration of interpreted topology is shown in Figure 6(c).

In the second example, the topology optimization problem was solved considering $w = 0.5$. The β coefficient was set equal to 0.0 and 0.0001 which means that the coupling constraint is not considered in the first case, and it is considered in the second case, respectively. The obtained piezoelectric FGM topologies are shown in Figures 7(a) and 8(a), respectively. The material gradation in the FGM domain along the 3 direction are shown in graphics of Figures 7(b) and 8(b), respectively. Again, a clear contrast among piezoelectric FGM topology and void could be obtained in both cases. The corresponding deformed configuration of interpreted topologies (considering 500 V/mm) are shown in Figures 7(c) and 8(c), respectively. For β equal to 0.0 the piezoceramic is distributed in the upper and lower parts of the design domain, like in the previous example. However, for β equal to 0.0001 the piezoceramic is distributed in lower part.

Table 2. Vertical displacement at point A (500 V/mm applied) and coupling factor (R_{yx}).

Piezoactuator	$u_y(\mu m)$	$u_x(\mu m)$	$R_{yx}(\%)$	w	β
Figure 6(a)	1.87	0.98	52.4	0.7	0.0
Figure 7(a)	1.12	0.80	71.4	0.5	0.0
Figures 8(a)	0.89	0.001	0.6	0.5	10^{-4}

Table 2 describes vertical displacement at point A (see Figure 5) considering $500 V/mm$ applied to the piezoceramic finite elements, and the coupling factor R_{xy} which is the ratio between undesired (horizontal) and desired (vertical) displacement. The largest displacement value is obtained for the first example, as expected, due to the large w value (w equal to 0.7), however, a large coupling was also obtained. For the second example,

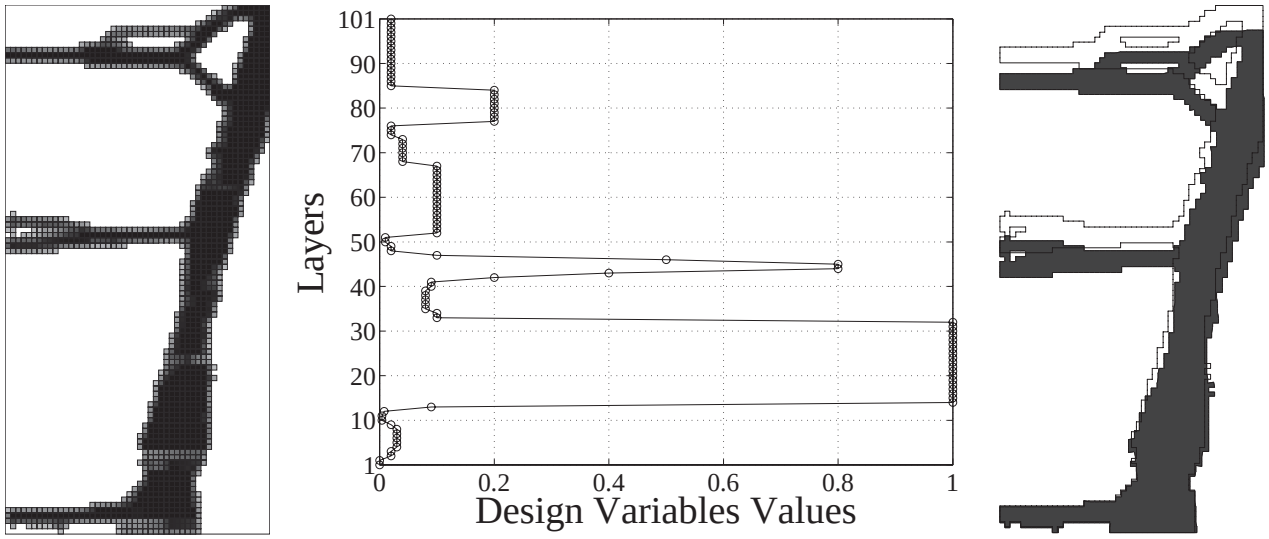

(a) (b) (c)

Figure 8. Result for $w = 0.5$ and $\beta = 0.0001$; a) Optimal topology; b) Material gradation along 3 direction; c) Deformed configuration of interpreted topology.

a smaller displacement was obtained due to lower value of w (0.5), however, for β equal to 0.0001 a negligible coupling was achieved.

6. CONCLUSIONS

A topology optimization formulation was proposed which allows the search of an optimal topology of a FGM piezoelectric structure for designing piezoelectric actuators, to achieve certain specified actuation movements. This is achieved by the optimization problem by allowing the simultaneous distribution of void and FGM piezoelectric in the design domain and applying an electric field as electrical excitation. The composition of FGM piezoelectric may include non-piezoelectric material. The adopted material model in the formulation is based on the density method and it interpolates fictitious densities at each finite element based on pseudo-densities defined as design variables for each finite element node providing a continuous material distribution in the domain. Some 2D examples were presented to illustrate the potentiality of the method. By controlling topology and material gradation large displacement and low displacement coupling constraint can be obtained. However, the optimization tends to give results with a steep material gradation in the FGM domain which suggests that some kind of gradation control must be implemented to allow the FGM gradation control, mainly for manufacturing purposes.

In future work, the designed piezoelectric actuators will be manufactured in a mesoscale by using a spark plasma sintering (SPS) machine, and displacement measurements will be conducted to verify the performance of these designs.

Acknowledgements

The first author thanks CNPq (Conselho Nacional de Desenvolvimento Científico e Tecnológico - Brazil), for supporting him through a doctoral fellowship ($n.^o 140687/2003-3$). The last author thanks FAPESP (Fundação de Amparo à Pesquisa do Estado de São Paulo – project $n.^o 06/57805-7$), CNPq, and the University of Illinois at Urbana-Champaign (UIUC) for inviting him as a Visiting Professor during the Summer/2006. We gratefully acknowledge the USA NSF through the project CMS#0303492 (Inter-Americas Collaboration in Materials Research and Education, PI Prof. W. Soboyejo, Princeton University).

REFERENCES

1. H. Ishihara, F. Arai, and T. Fukuda, "Micro mechatronics and micro actuators," *IEEE/ASME Transactions on Mechatronics* **1**(1), pp. 68–79, 1996.
2. P. F. Indermuhle, V. Jaecklin, J. Brugger, C. Linder, N. D. Rooij, and M. Binggeli, "Afm imaging with an xy – micropositioner with integrated tip," *Sensors and Actuators A: Physical* **47**(1–3), pp. 562–565, 1995.
3. S. Ku, U. Pinsopon, S. Cetinkunt, and S. Nakajima, "Design, fabrication, and real-time neural network control of a three-degrees-of-freedom nanopositioner," *IEEE/ASME Transactions on Mechatronics* **5**(3), pp. 273–279, 2000.
4. R. Pérez, J. Agnus, C. Clévy, A. Hubert, and N. Chaillet, "Modeling, fabrication, and validation of a high-performance 2-dof piezoactuator for micromanipulation," *IEEE/ASME Transactions on Mechatronics* **10**(2), pp. 161–171, 2005.
5. A. Menciassi, A. Eisinberg, M. C. Carrozza, and P. Dario, "Force sensing microinstrument for measuring tissue properties and pulse in microsurgery," *IEEE/ASME Transactions on Mechatronics* **8**(1), pp. 10–17, 2003.
6. L. L. Howell, *Compliant Mechanisms*, John Wiley & Sons, Inc., New York, USA, 2001.
7. S. Canfield and M. I. Frecker, "Topology optimization of compliant mechanical amplifiers for piezoelectric actuators," *Structural and Multidisciplinary Optimization* **20**, pp. 269–279, 2000.
8. R. C. Carbonari, E. C. N. Silva, and S. Nishiwaki, "Design of piezoelectric multiactuated microtools using topology optimization," *Smart Materials and Structures* **14**, pp. 1431–1447, 2005.
9. R. C. Carbonari, E. C. N. Silva, and S. Nishiwaki, "Optimum placement of piezoelectric material in the piezoactuator design," *Smart Materials and Structures* **in press**, 2006.
10. Y. Miyamoto, W. A. Kaysser, B. H. Rabin, A. Kawasaki, and R. G. Ford, *Functionally Graded Materials: Design, Processing and Applications*, Kluwer Academic Publishers, Dordrecht, 1999.
11. M. P. Bendsøe and O. Sigmund, *Topology Optimization - Theory, Methods and Applications*, Springer, New York, EUA, 2003.
12. S. Turteltaub, "Functionally graded materials for prescribed field evolution," *Computer Methods in Applied Mechanics and Engineering* **191**, pp. 2283–2296, 2002.
13. G. H. Paulino and E. C. N. Silva, "Design of functionally graded structures using topology optimization," *Materials Science Forum* **492–493**, pp. 435–440, 2005.
14. A. Almajid, M. Taya, and S. Hudnut, "Analysis of out-of-plane displacement and stress field in a piezocomposite plate with functionally graded microstructure," *International Journal of Solids and Structures* **38**(19), pp. 3377–3391, 2001.
15. S. Zhifei, "General solution of a density functionally gradient piezoelectric cantilever and its applications," *Smart materials and Structures* **11**, pp. 122–129, 2002.
16. G. N. Vanderplaatz, *Numerical Optimization Techniques for Engineering Design: with Applications*, McGraw-Hill, New York, USA, 1984.
17. R. Hanson and K. Hiebert, *A Sparse Linear Programming Subprogram*, Sandia National Laboratories, Technical Report SAND81-0297, 1981.
18. R. Lerch, "Simulation of piezoelectric devices by two-and three-dimensional finite elements," *IEEE Transactions on Ultrasonics, Ferroelectrics and Frequency Control* **37**(2), pp. 233–247, 1990.
19. J. H. Kim and G. H. Paulino, "Isoparametric graded finite elements for nonhomogeneous isotropic and orthotropic materials," *ASME Journal of Applied Mechanics* **69**(4), pp. 502–514, 2002.
20. K. Matsui and K. Terada, "Continuous approximation of material distribution for topology optimization," *International Journal for Numerical Methods in Engineering* **59**(14), pp. 1925–1944, 2004.
21. E. C. N. Silva, S. Nishiwaki, and N. Kikuchi, "Topology optimization design of flextensional actuators," *IEEE Transactions on Ultrasonics, Ferroelectrics and Frequency Control* **47**(3), pp. 657–671, 2000.